Description of the crystal structure

The complex [Ni(pydc)(pydm)]·H_2O crystallizes in the monoclinic system with the space group $P2_1/c$. Its crystal structure consists of complex molecules of [Ni(pydc)(pydm)] and uncoordinated water molecules. The Ni(II) central atom is hexacoordinated by two carboxylato oxygen atoms [Ni1–O1 = 2.119(4) Å, Ni1–O3 = 2.151(4) Å] and one pyridine nitrogen atom [Ni1–N1 = 1.962(5) Å] from the tridentate dipicolinato ligand, and two hydroxyl oxygen atoms [Ni1–O5 = 2.110(4) Å, Ni1–O6 = 2.138(4) Å] and one pyridine nitrogen atom [Ni1–N2 = 1.992(5) Å] from the tridentate pyridine-2,6-dimethanol. The complex molecules and uncoordinated water molecules are linked to 2-D supramolecular frameworks through hydrogen bonds between hydroxyl oxygen atoms of the pyridine-2,6-dimethanol and uncoordinated carboxylato oxygen atoms of dipicolinato ligands [O5–H5O···O4 with O5···O4 distance of 2.622(6) Å], between hydroxyl oxygen atoms of pyridine-2,6-dimethanol and uncoordinated water molecules [O6–H6O···O1W with O6···O1W distance of 2.656(6) Å], between uncoordinated water molecules and carboxylato oxygen atoms of dipicolinato ligands [O1W–H1W···O1, O1W–H2W···O5 with O···O distances of 2.700(6) and 2.985(6) Å, respectively] and form double layers. In the crystal structure of **1** the π-π stacking interactions are observed between pyridine rings of pyridine-2,6-dimethanol with $c_g \cdots c_g$ distances of 3.58 and 3.40 Å and shift-distances of 1.77 and 1.23 Å (for detail see ref. [1]).

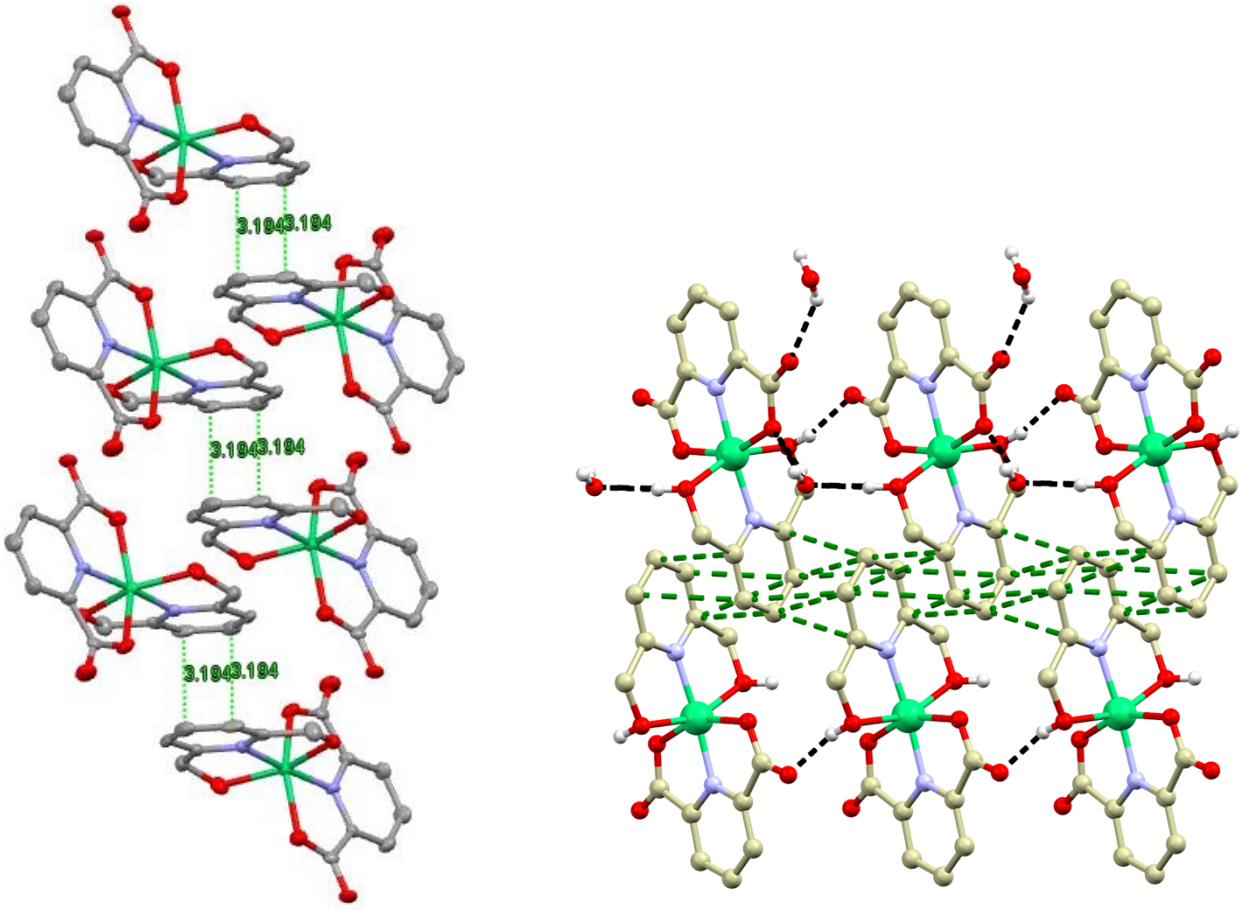

Fig. S1. Zoomed view to the crystal structure of **1**.

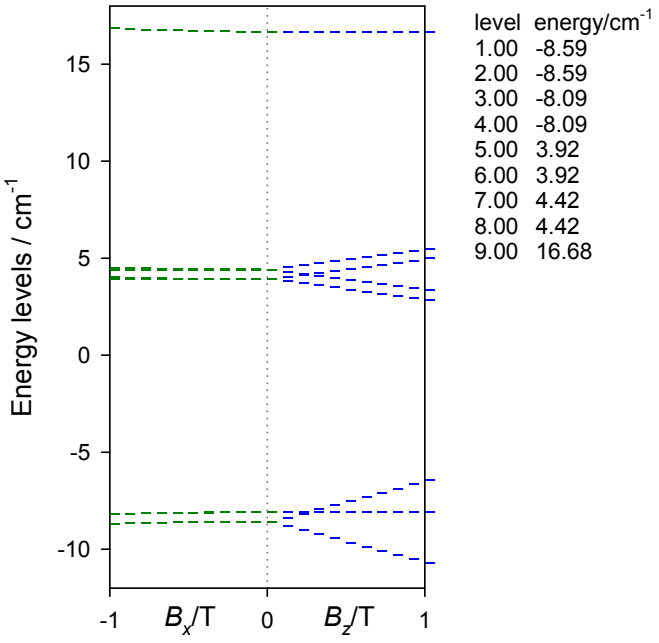

Fig. S2. Calculated energy levels for a dimeric $[\mathbf{1}]_2$ complex in the weak exchange limit using the spin Hamiltonian formalism. Magnetic parameters resulting from the magnetic data fitting: J/hc = +0.25 cm^{-1}, g_z = 2.289, g_x = 2.277, D/hc = -12.5 cm^{-1}, χ_{TIM} = 0.99 × 10^{-9} m^3 mol^{-1}, zj/hc = -0.039 cm^{-1}; $R(\chi)$ = 0.010, $R(M)$ = 0.030.

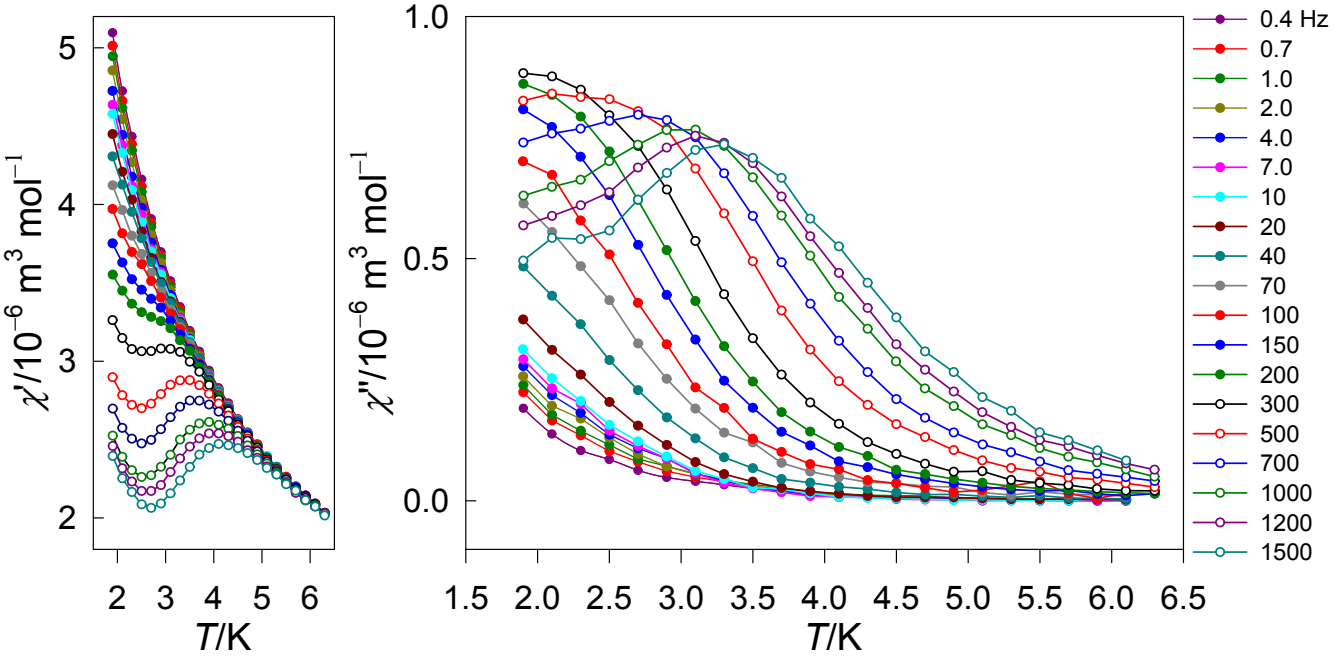

Figure S3. The in-phase χ' and out-of-phase χ'' molar susceptibility (SI units) for **1** at the applied external field B_{DC} = 0.2 T. Lines serve as a guide for eyes.

Table S1. Parameters of the extended Debye model for **1** (two relaxation processes) at B_{DC} = 0.2 T.

T/K	χ_S	χ_{T1}	α_1	τ_1 /10^{-3} s	χ_{T2}	α_2	τ_2 /10^{-3} s	$R(\chi')$/%	$R(\chi'')$/%
1.9	2.08(1)	4.42(3)	0.20(1)	0.542(5)	5.33(3)	0.42(3)	91(6)	0.18	0.82
2.1	1.93(1)	4.16(5)	0.17(1)	0.480(6)	4.94(5)	0.48(5)	77(11)	0.29	1.21
2.3	1.80(1)	4.04(3)	0.17(1)	0.432(6)	4.53(3)	0.34(6)	74(9)	0.40	0.93
2.5	1.73(1)	3.85(1)	0.16(1)	0.363(3)	4.23(2)	0.34(5)	90(19)	0.26	0.95
2.7	1.64(1)	3.68(1)	0.15(1)	0.286(2)	3.96(2)	0.34(6)	81(10)	0.29	0.50
2.9	1.58(1)	3.53(1)	0.13(1)	0.225(2)	3.74(1)	0.27(6)	80(10)	0.30	0.74
3.1	1.51(2)	3.39(1)	0.13(1)	0.171(2)	3.54(2)	0.28(8)	116(22)	0.26	0.91
3.3	1.53(2)	3.26(1)	0.10(1)	0.136(2)	3.38(2)	0.29(11)	131(40)	0.30	1.00
3.5	1.48(3)	3.13(1)	0.10(1)	0.106(3)	3.22(2)	0.20(16)	169(66)	0.29	1.49
3.7	1.56(3)	3.01(1)	0.06(1)	0.093(3)	3.09(3)	0.33(20)	224(180)	0.31	0.84
4.1	1.39(6)	2.80(1)	0.07(1)	0.053(3)	2.83(1)	0.05(30)	252(162)	0.27	1.40
5.1	1.82(9)	2.39(1)	0.01(4)	0.050(10)	-	-	-	0.47	3.7
6.1	1.85(5)	2.08(1)	0	0.049(11)	-	-	-	0.71	8.0

[a] SI unit for the molar magnetic susceptibility [10^{-6} m^3 mol^{-1}]. Standard deviations in parentheses (last digit). R – discrepancy factor of the fit for dispersion χ' and absorption χ'', respectively.

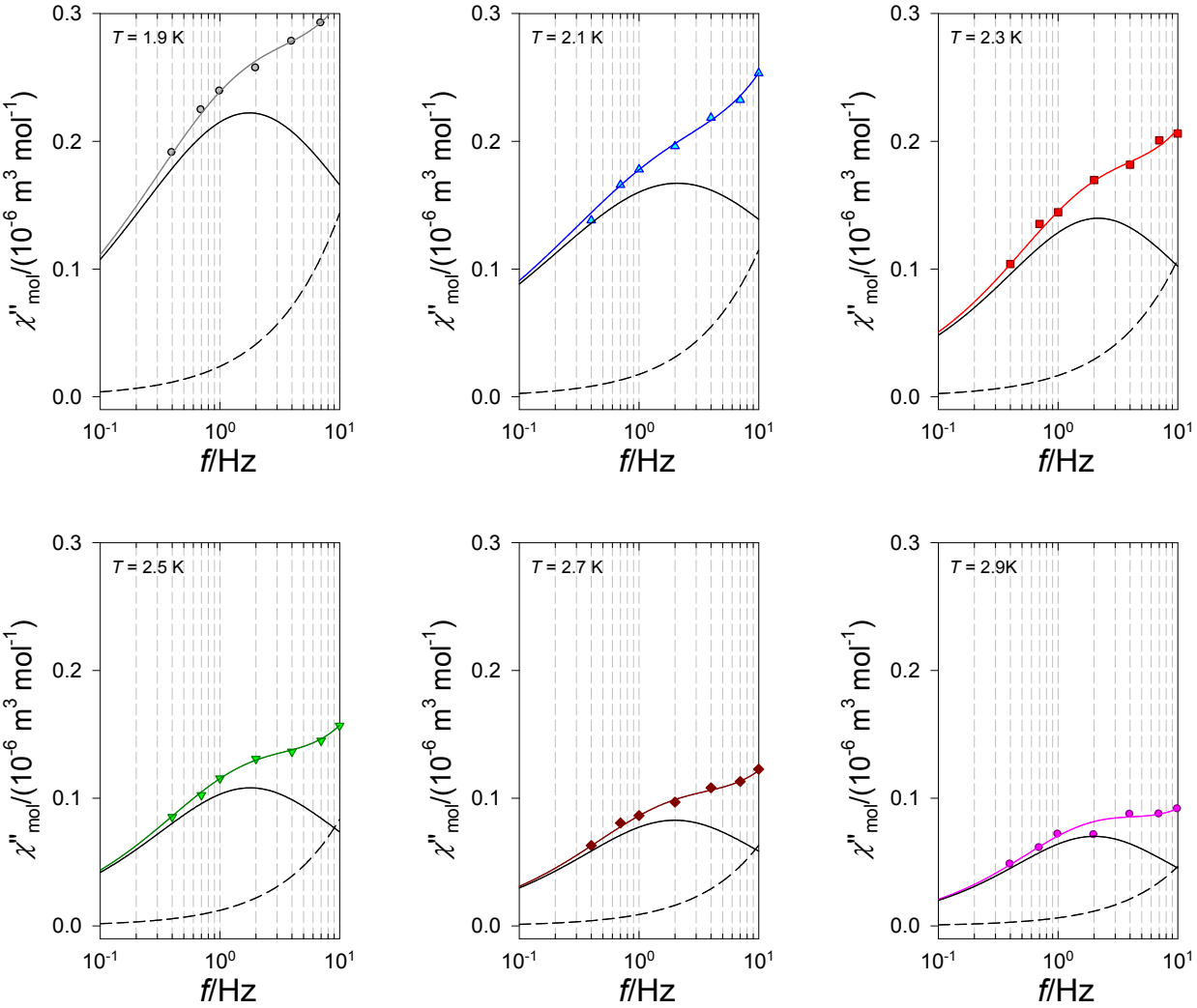

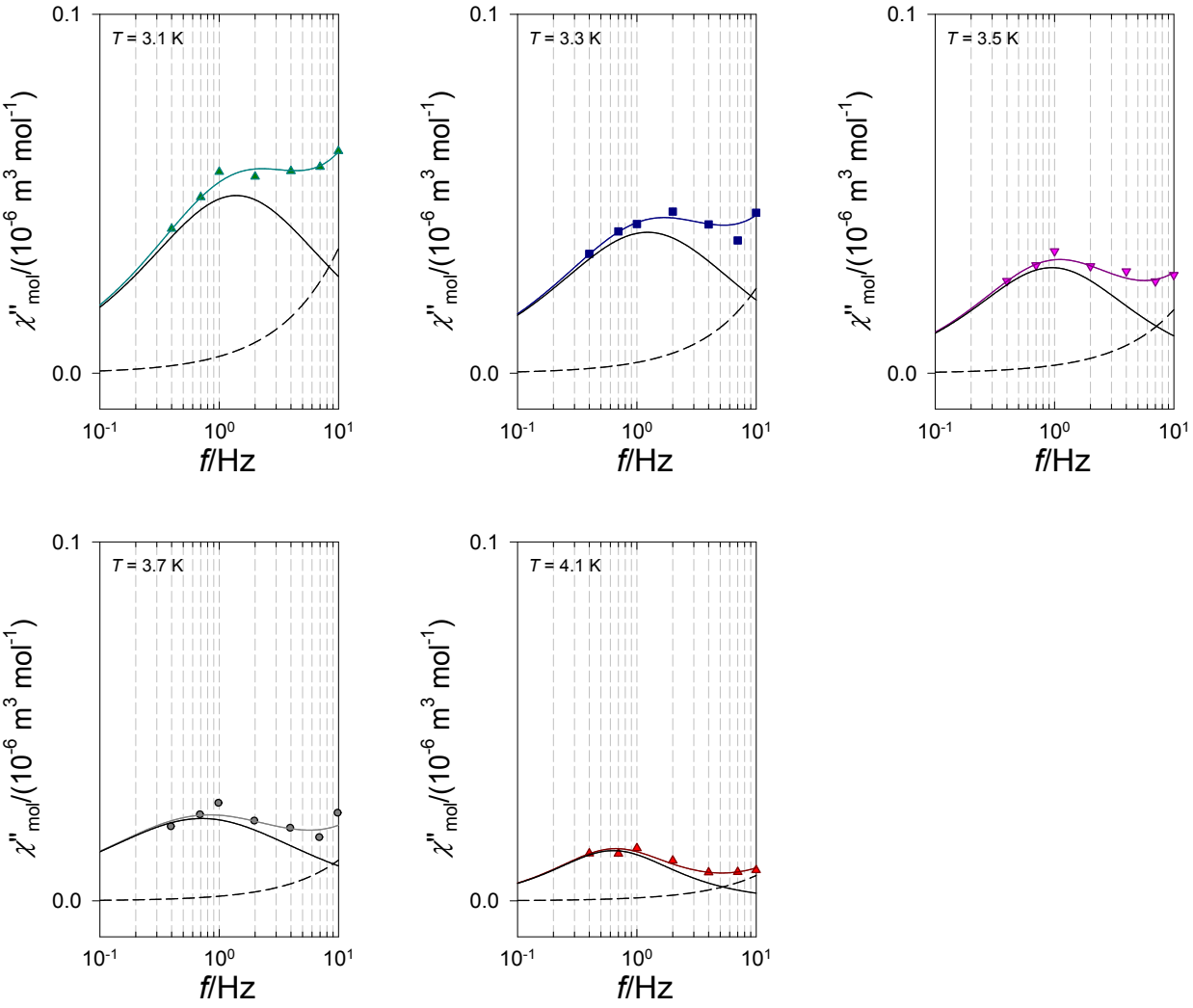

Fig. S4. Deconvolution lines of the fitted χ'' *vs f* curves in the low-frequency window.

Doping experiments

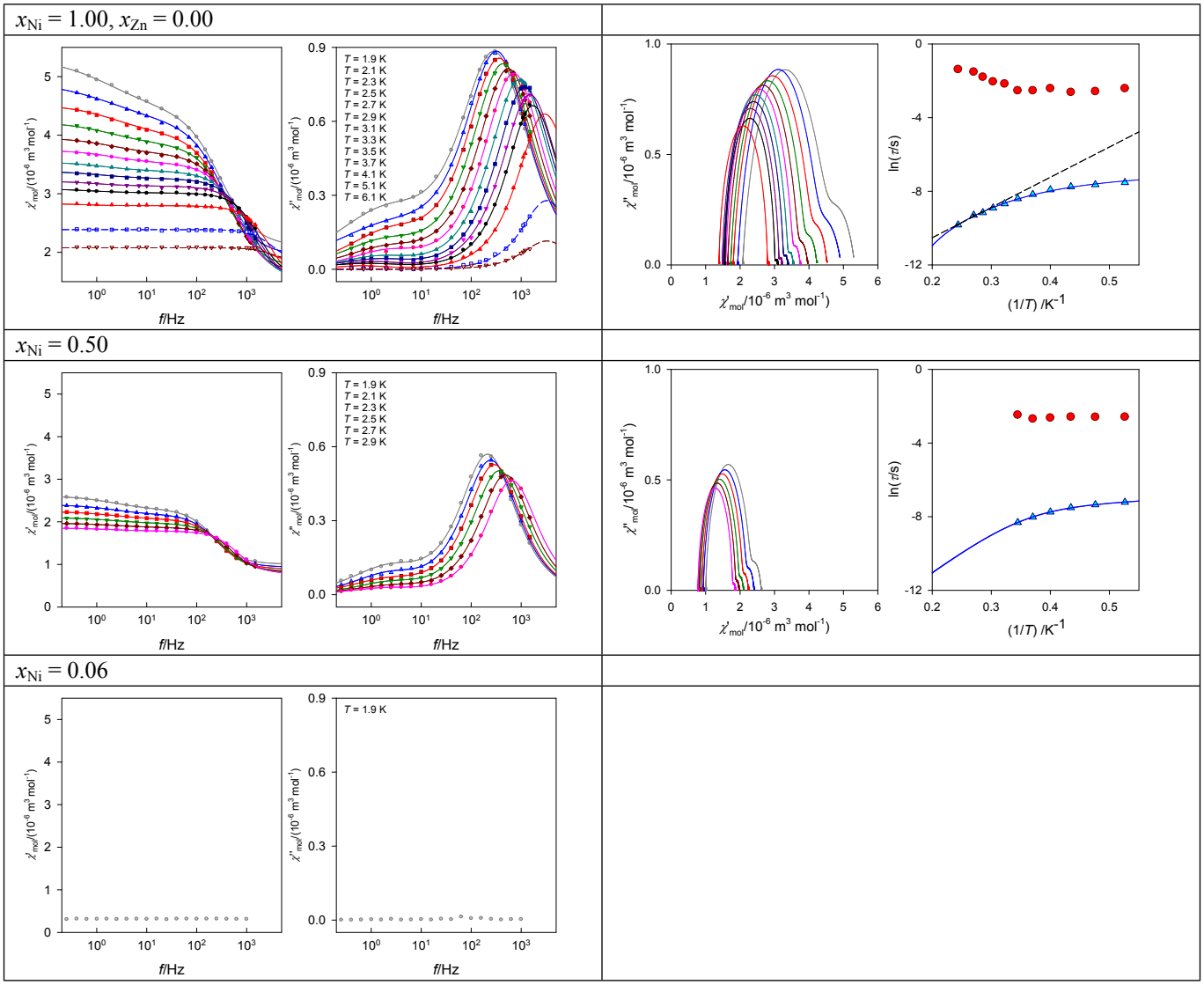

Fig. S5. Comparison of the AC susceptibility measurements for various degrees of Ni:Zndoping.

Table S2. Parameters of the extended Debye model for **2** (two relaxation processes) at B_{DC} = 0.2 T.

T/K	χ_S	χ_{T1}	α_1	τ_1 /10^{-3} s	χ_{T2}	α_2	τ_2 /10^{-3} s	$R(\chi')$/%	$R(\chi'')$/%
1.9	1.00(1)	2.29(1)	0.09(1)	0.73(1)	2.61(1)	0.27(2)	76(4)	0.26	1.8
2.1	0.93(1)	2.17(1)	0.09(1)	0.64(1)	2.40(1)	0.24(3)	75(5)	0.28	1.7
2.3	0.89(1)	2.06(1)	0.07(1)	0.55(1)	2.24(1)	0.27(3)	75(6)	0.25	1.5
2.5	0.84(1)	1.96(1)	0.07(1)	0.43(1)	2.10(1)	0.23(4)	72(6)	0.31	1.2
2.7	0.80(1)	1.86(1)	0.05(1)	0.33(1)	1.97(1)	0.28(4)	68(7)	0.24	1.3
2.9	0.78(1)	1.78(1)	0.05(1)	0.24(1)	1.86(1)	0.24(5)	85(9)	0.25	0.73

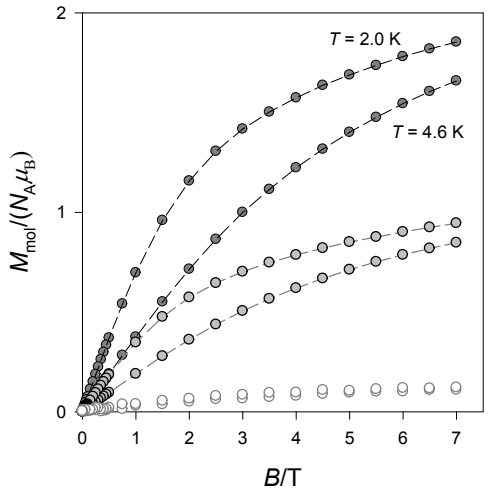

Fig. S6. DC magnetization per formula unit for Ni:Zn doped materials with the mole fraction x_{Ni} = 1.00 (dark gray), 0.50 (gray), and 0.06 (white).

Ab Initio Calculations

Quantum-chemical calculations of the ZFS based on X-ray diffraction-determined structure were performed with the ORCA program [2]. For this purpose, an *ab initio* wave function based method has been chosen, such as complete active space self-consistent field (CASSCF) improved with the second-order *N*-electron valence perturbation theory (NEVPT2). An active space in which eight electrons are distributed into the five nickel d-orbitals (CAS(8,5)) was employed along with the TZVP basis set for all elements. In CASSCF procedure, the orbitals were optimized for the average of 10 triplet (^{3}F and ^{3}P terms of the free Ni(II)) and 15 singlet (^{1}G, ^{1}D and ^{1}S terms) roots. The state-averaged (SA) CASSCF calculations were performed on top of quasi-restricted DFT/BP86/TZVP orbitals. The *D*-values were calculated through quasi-degenerate perturbation theory (QDPT) in which the spin-orbit coupling (SOC) operator (in SOMF approximation) is diagonalized in the basis of the non-relativistic SA-CASSCF/NEVPT2 eigenfunctions [3]. Diagonalization of the resulting matrix yields the energy levels and eigenvectors of the coupled states that were used for constructing the *D*-tensor through the formalism based on effective Hamiltonian approach.

Table S3. Calculated CAS(8,5)/NEVPT2 transition energies and SOC splitting of the ground state for the complex **1**.

Root	Multiplicity	ΔE/cm^{-1}	ΔE^{SOC}/cm^{-1}
0	3	0	0, 9.0, 19.9
1	3	6956	
2	3	9306	
3	3	11029	
0	1	13596	
4	3	15006	
1	1	16483	
5	3	17026	
6	3	17725	
2	1	22969	
3	1	24741	
7	3	25315	
4	1	26082	
8	3	28218	
5	1	29212	
6	1	29792	
9	3	30228	
7	1	33306	
8	1	35426	
9	1	37534	
10	1	37761	
11	1	38760	
12	1	39909	
13	1	40462	
14	1	69013	

Table S4. Individual contributions to D and E of the excited triplet and singlet states computed at the CAS(8,5)/NEVPT2 level for the complex **1**.

Root	Multiplicity	D/cm^{-1}	E/cm^{-1}
1	3	–60.33	–0.02
2	3	21.42	–16.81
3	3	16.50	11.46
4	3	1.22	–0.34
5	3	0.79	–0.03
6	3	0	0.13
7	3	0.08	0.07
8	3	0.05	–0.04
9	3	–0.02	0
0	1	0.30	0
1	1	0.03	0
2	1	16.29	–0.01
3	1	–6.63	5.31
4	1	–5.44	–4.42
5	1	–1.12	–0.60
6	1	0.10	0
7	1	–0.28	0.28
8	1	–0.02	–0.02
9	1	0.80	0
10	1	0.02	0.01
11	1	–1.06	–0.44
12	1	0.40	0.01
13	1	–0.79	0.31
14	1	0.01	0

References

[1] J. Miklovič, A. Packová, P. Segľa, J. Titiš, M. Koman, J. Moncoľ, R. Boča, V. Jorík, H. Krekuska, D. Valigura, Inorg. Chim. Acta, 2015, 429, 73.

[2] (a) Neese, F. ORCA – An Ab Initio, Density Functional and Semi-empirical Program Package, Version 3.0.3. (b) Atanasov, M.; Ganyushin, D.; Pantazis, D. A.; Sivalingam, K.; Neese, F. Inorg. Chem. 2011, 50, 7460. (c) Angeli, C.; Borini, S.; Cestari, M.; Cimiraglia, R. J. Chem. Phys. 2004, 121, 4043. (d) Angeli, C.; Cimiraglia, R.; Evangelisti, S.; Leininger, T.; Malrieu, J.–P. J. Chem. Phys. 2001, 114, 10252. (e) Angeli, C.; Cimiraglia, R.; Malrieu, J.–P. J. Chem. Phys. 2002, 117, 9138.

[3] (a) Neese, F. J. Chem. Phys. 2005, 122, 34107. (b) Ganyushin, D.; Neese, F. J. Chem. Phys. 2006, 125, 24103. (c) Neese, F. J. Chem. Phys. 2007, 127, 164112.